

Photocontrol of the Supramolecular Chirality Imposed by Stereocenters in Liquid Crystalline Azodendrimers

Jesús del Barrio,[†] Rosa M. Tejedor,[†] Luiz S. Chinelatto,[†] Carlos Sánchez,[‡] Milagros Piñol,[†] and Luis Oriol^{*,†}

[†]Departamento de Química Orgánica y Química Física and [‡]Departamento de Física de la Materia Condensada, Facultad de Ciencias-Instituto de Ciencia de Materiales de Aragón, Universidad de Zaragoza-CSIC, 50009 Zaragoza, Spain

Received October 9, 2009. Revised Manuscript Received December 15, 2009

A series of liquid crystalline dendrimers have been synthesized by peripheral functionalization of PPI dendrimers (generations having 16 or 32 functional groups) with photochromic azobenzene units that contain stereocenters at the terminal alkyl chains. Complete functionalization was checked by NMR and MALDI-TOF mass spectrometry. The mesomorphic properties were analyzed by optical microscopy, DSC, X-ray diffraction and AFM. The dendrimers exhibit a smectic phase that can be frozen at room temperature depending on the thermal history of the sample. Dendrimers did not exhibit a CD response in solution. However, chiroptical properties were detected in films and these were assigned to a supramolecular chirality arising from aggregation of azobenzene units and imposed by the stereocenters. The chiroptical properties depend to a small extent on the thermal history of the sample and can be modulated with light. For example, irradiation with UV light erases the CD signal of the films due to trans–cis isomerization, but this eventually reverts to the initial CD signal by cis–trans back isomerization and aggregation. Irradiation with 488 nm circular polarized light (CPL) modulates the CD signal depending on the handedness of the light and generation of dendrimeric core. Irradiation with l-CPL reinforces the supramolecular chirality imposed by stereocenters in both dendrimers. However, irradiation with r-CPL switches the CD signal in films of the generation dendrimer having 16 functional groups, **G2-AZO-C4(S)**, but this does not occur in films of the higher generation dendrimer, **G3-AZO-C4(S)**.

Introduction

Dendrimers, such as poly(propylene imine) (PPI) or poly(amido amine) (PAMAM), have a controlled structure that consists of an internal core surrounded by a branched shell with a well-defined number of reactive groups at the periphery and these can be chemically modified in order to introduce active molecules.¹ This approach can be used to obtain nanometer-sized functional molecules and for applications in fields ranging from medicine^{2–5} to materials science and engineering.^{6–8} For instance, photoactive moieties can be incorporated into dendritic structures resulting in materials that have unique photochemical and photophysical properties.

These properties are easy to manipulate by controlling the number, type, and location of active units linked to the dendritic architecture.^{9,10} Within the field of photoactive materials, azobenzene-containing systems have been the subject of intense research activity as the trans–cis reversible photoisomerization of azobenzenes is the origin of a large number of applications, particularly in azobenzene-containing polymers or azopolymers. These applications range from optical storage media to photomechanical actuators.^{11–13}

Most azopolymers are based on conventional polymers (e.g., polymethacrylates) with pendant azobenzene units. Dendrimers with photochromic azobenzene units or azodendrimers represent an interesting alternative to those conventional linear polymers. Despite the novelty of photochromic dendrimers, a significant number of

*Corresponding author. Fax +34 976762086. E-mail: loriol@unizar.es.
(1) Vögtle, F.; Richardt, G.; Werner, N., *Dendrimer Chemistry. Concepts, Syntheses, Properties, Applications*; Wiley-VCH: Weinheim, Germany, 2009; p 342.
(2) Tekade, R. K.; Kumar, P. V.; Jain, N. K. *Chem. Rev.* **2009**, *109*, 49–87.
(3) Medina, S. H.; El-Sayed, M. E. H. *Chem. Rev.* **2009**, *109*, 3141–3157.
(4) Bharali, D. J.; Khalil, M.; Gurbuz, M.; Simone, T. M.; Mousa, S. A. *Int. J. Nanomed.* **2009**, *4*, 1–7.
(5) Gao, Y.; Gao, G.; He, Y.; Liu, T. L.; Qi, R. *Mini Rev. Med. Chem.* **2008**, *8*, 889–900.
(6) Hwang, S. H.; Moorefield, C. N.; Newkome, G. R. *Chem. Soc. Rev.* **2008**, *37*, 2543–2557.
(7) Luo, J. D.; Ma, H.; Jen, A. K. Y. *C. R. Chim.* **2003**, *6*, 895–902.
(8) Hecht, S.; Frechet, J. M. J. *Angew. Chem., Int. Ed.* **2001**, *40*, 74–91.

(9) D'Ambruoso, G. D.; McGrath, D. V., Energy Harvesting in Synthetic Dendrimer Materials. In *Photoresponsive Polymers II*; Springer: New York, 2008; Vol. 214, pp 87–147.
(10) Balzani, V.; Ceroni, P.; Maestri, M.; Saudan, C.; Vicinelli, V. *Dendrimers V: Functional and Hyperbranched Building Blocks, Photophysical Properties, Applications in Materials and Life Sciences*; Springer: New York, 2003; Vol. 228, pp 159–191.
(11) Natansohn, A.; Rochon, P. *Chem. Rev.* **2002**, *102*, 4139–4175.
(12) Matharu, A. S.; Jeeva, S.; Ramanujam, P. S. *Chem. Soc. Rev.* **2007**, *36*, 1868–1880.
(13) Ikeda, T.; Mamiya, J.; Yu, Y. L. *Angew. Chem., Int. Ed.* **2007**, *46*, 506–528.

azodendrimers have been reported and these are claimed to have potential applications as photoswitchable hosts,¹⁴ harvesting systems,¹⁵ or holographic recording media.¹⁶ Dendrimers and dendrons have been reported in which the photoisomerizable moieties are located either in the interior or at the surface of the macromolecule.^{17–19} However, from the synthetic point of view, the simplest and most straightforward route toward the functionalization of dendrimers is the chemical modification of the surface of a preformed dendritic skeleton with peripheral functional groups. In this way, the incorporation of photoactive units can result in materials with a very dense distribution of disentangled functional moieties that provide easily tunable photochemical and/or photophysical properties. Nevertheless, most of the literature reports concerning dendrimers with peripheral azobenzene groups describe their photophysical and photochemical properties in solution. It seems that the photoisomerization of peripheral azobenzenes is not perturbed by their attachment to the dendrimer. Less work has been devoted to exploring the photoresponsive properties of these systems in films. Aggregation phenomena and their influence on photoisomerization or photoalignment in thin films have been addressed by different authors.^{20,21} Besides, photomanipulation of azobenzenes aggregation has been also investigated in supramolecular assemblies.^{22–26} In the case of dendrimers, the photoalignment under irradiation with linearly polarized light has been investigated in films of liquid crystalline dendrimers such as carbosilane dendrimers with 4-alkoxyazobenzene covalently attached to the surface^{27,28} and also poly(propylene imine) (PPI) or poly(amidoamine) liquid crystalline dendrimers with covalently or ionically bonded 4-cyanoazobenzene moieties.^{29,30} Formation of surface relief gratings is an interesting property of azopolymers that has also been investigated in dendrimers

(14) Puntoriero, F.; Ceroni, P.; Balzani, V.; Bergamini, G.; Vogtle, F. *J. Am. Chem. Soc.* **2007**, *129*, 10714–10719.

(15) Jiang, D. L.; Aida, T. *Nature* **1997**, *388*, 454–456.

(16) Archut, A.; Vogtle, F.; De Cola, L.; Azzellini, G. C.; Balzani, V.; Ramanujam, P. S.; Berg, R. H. *Chem.—Eur. J.* **1998**, *4*, 699–706.

(17) Shen, X.; Liu, H.; Li, Y.; Liu, S. *Macromolecules* **2008**, *41*, 2421–2425.

(18) Liao, L.-X.; Stellacci, F.; McGrath, D. V. *J. Am. Chem. Soc.* **2004**, *126*, 2181–2185.

(19) Li, S.; McGrath, D. V. *J. Am. Chem. Soc.* **2000**, *122*, 6795–6796.

(20) Nithyanandhan, J.; Jayaraman, N.; Davis, R.; Das, S. *Chem.—Eur. J.* **2004**, *10*, 689–698.

(21) Patton, D.; Park, M. K.; Wang, S. X.; Advincula, R. C. *Langmuir* **2002**, *18*, 1688–1694.

(22) Murata, K.; Aoki, M.; Suzuki, T.; Harada, T.; Kawabata, H.; Komori, T.; Ohseto, F.; Ueda, K.; Shinkai, S. *J. Am. Chem. Soc.* **1994**, *116*, 6664–6676.

(23) Song, X. D.; Perlstein, J.; Whitten, D. G. *J. Am. Chem. Soc.* **1997**, *119*, 9144–9159.

(24) Weener, J. W.; Meijer, E. W. *Adv. Mater.* **2000**, *12*, 741–746.

(25) Zhang, Y.; Chen, P.; Liu, M. *Langmuir* **2006**, *22*, 10246–10250.

(26) Zhang, W. Q.; Xie, J. D.; Yang, Z.; Shi, W. F. *Polymer* **2007**, *48*, 4466–4481.

(27) Bobrovsky, A.; Ponomarenko, S.; Boiko, N.; Shibaev, V.; Rebrov, E.; Muzaferov, A.; Stumpe, J. *Macromol. Chem. Phys.* **2002**, *203*, 1539–1546.

(28) Bobrovsky, A. Y.; Pakhomov, A. A.; Zhu, X. M.; Boiko, N. I.; Shibaev, V. P.; Stumpe, J. *J. Phys. Chem. B* **2002**, *106*, 540–546.

(29) Alcalá, R.; Giménez, R.; Oriol, L.; Piñol, M.; Serrano, J. L.; Villacampa, B.; Viñuales, A. I. *Chem. Mater.* **2007**, *19*, 235–246.

(30) Marcos, M.; Alcalá, R.; Barberá, J.; Romero, P.; Sánchez, C.; Serrano, J. L. *Chem. Mater.* **2008**, *20*, 5209–5217.

(31) He, Y. N.; Gu, X. Y.; Guo, M. C.; Wang, X. G. *Opt. Mater.* **2008**, *31*, 18–27.

(32) Del Barrio, J.; Oriol, L.; Alcalá, R.; Sánchez, C. *Macromolecules* **2009**, *42*, 5752–5760.

(33) Nikolova, L.; Todorov, T.; Ivanov, M.; Andruzz, F.; Hvilsted, S.; Ramanujam, P. S. *Opt. Mater.* **1997**, *8*, 255–258.

(34) Naydenova, I.; Nikolova, L.; Ramanujam, P. S.; Hvilsted, S. *J. Opt. A: Pure Appl. Opt.* **1999**, *1*, 438–441.

(35) Ivanov, M.; Naydenova, I.; Todorov, T.; Nikolova, L.; Petrova, T.; Tomova, N.; Dragostinova, V. *J. Mod. Opt.* **2000**, *47*, 861–867.

(36) Nedelchev, L.; Nikolova, L.; Todorov, T.; Petrova, T.; Tomova, N.; Dragostinova, V.; Ramanujam, P. S.; Hvilsted, S. *J. Opt. A: Pure Appl. Opt.* **2001**, *3*, 304–310.

(37) Nedelchev, L.; Nikolova, L.; Matharu, A.; Ramanujam, P. S. *Appl. Phys. B: Laser Opt.* **2002**, *75*, 671–676.

(38) Cipparrone, G.; Pagliusi, P.; Provenzano, C.; Shibaev, V. P. *Macromolecules* **2008**, *41*, 5992–5996.

(39) Iftime, G.; Labarthe, F. L.; Natansohn, A.; Rochon, P. *J. Am. Chem. Soc.* **2000**, *122*, 124646–12650.

(40) Wu, Y.; Natansohn, A.; Rochon, P. *Macromolecules* **2004**, *37*, 6801–6805.

(41) Hore, D. K.; Natansohn, A.; Rochon, P. *J. Phys. Chem. B* **2003**, *107*, 2506–2518.

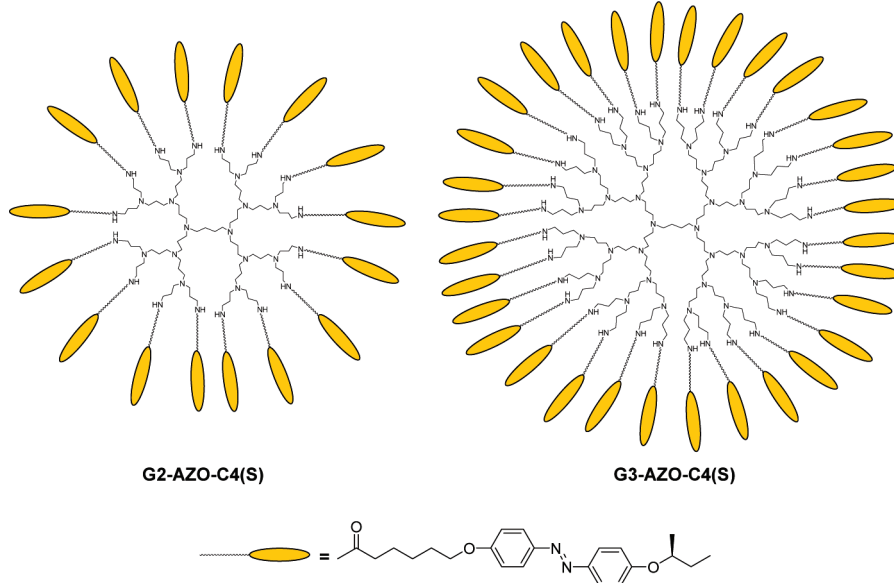
(42) Hore, D. K.; Wu, Y.; Natansohn, A.; Rochon, P. *J. Appl. Phys.* **2003**, *2003*, 2162–2166.

(43) Tejedor, R. M.; Millaruelo, M.; Oriol, L.; Serrano, J. L.; Alcalá, R.; Rodríguez, F. J.; Villacampa, B. *J. Mater. Chem.* **2006**, *16*, 1674–1680.

(44) Tejedor, R. M.; Oriol, L.; Serrano, J. L.; Partal-Ureña, F.; López-González, J. J. *Adv. Funct. Mater.* **2007**, *17*, 3486–3492.

(45) Del Barrio, J.; Tejedor, R. M.; Chinelatto, L. S.; Sánchez, C.; Pinol, M.; Oriol, L. *J. Mater. Chem.* **2009**, *19*, 4922–4930.

Chart 1. Schematic Representation of the Photochromic Dendrimers



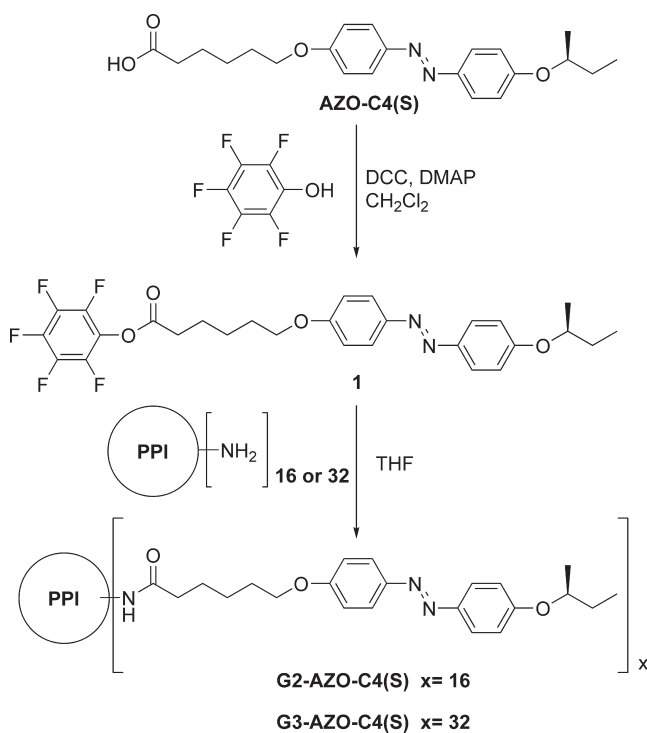
properties of the materials under investigation will be compared with results obtained on polymers with conventional side chain architecture. Stereocenters introduced in terminal alkyl chains can govern the chiral supramolecular arrangement of azobenzene units in the bulk material. Chiroptical properties associated with the chiral supramolecular organization of azobenzene mesogenic units will be described for dendritic films and the effects of thermal history and irradiation—either with unpolarized light or with circularly polarized light (CPL)—on these supramolecular organizations will be discussed. The influence of the dendritic structure on the switching and modulation of chiroptical properties by light will be analyzed.

Experimental Section

Materials. The starting PPI was purchased from Aldrich and was used without further purification. Synthesis of the target functionalized dendrimers was carried out according to the synthetic pathway shown in Scheme 1. The azobenzene-containing carboxylic acid **AZO-C4(S)** was synthesized according to a previously described method.⁴⁶

2,3,4,5,6-Pentafluorophenyl 6-[4'-(S)-methylpropoxyxyphe-nylazo]phenyloxyhexanoate (1). Pentafluorophenol (1.53 g, 8.30 mmol), **AZO-C4(S)** (2.90 g, 7.54 mmol) and *N,N*-dimethyl-4-aminopyridine (DMAP) (0.09 g, 0.75 mmol) were diluted in dry dichloromethane (250 mL). The reaction flask was flushed with argon and *N,N'*-dicyclohexylcarbodiimide (DCC) (1.56 g, 7.54 mmol) was added. The mixture was stirred at room temperature for 24 h. The precipitate (*N,N'*-dicyclohexylurea) was filtered off on a glass filter and washed with a small amount of dichloromethane. The combined organic fractions were evaporated in *vacuo* and the crude product was purified by flash column chromatography on silica gel eluting with CH_2Cl_2 to yield the required product as a yellow solid. Yield: 79% (3.28 g, 5.96 mmol). ^1H NMR (400 MHz, CDCl_3 , δ): 7.86 (dd, $J = 9.0, 3.6$ Hz, 4H), 6.98 (dd, $J = 9.0, 4.1$ Hz, 4H), 4.44–4.36 (m, 1H),

Scheme 1. Synthetic Pathway to the Photochromic Dendrimers



4.06 (t, $J = 6.3$ Hz, 2H), 2.72 (t, $J = 7.4$ Hz, 2H), 1.93–1.59 (m, 8H), 1.34 (d, $J = 6.1$ Hz, 3H) 1.00 (t, $J = 7.5$ Hz, 3H). ^{13}C NMR (100 MHz, CDCl_3 , δ): 169.4, 160.9, 160.4, 147.1, 146.8, 124.4, 124.3, 115.8, 114.6, 75.3, 67.8, 33.3, 29.2, 28.8, 25.5, 24.5, 19.3, 9.8. IR (KBr, cm^{-1}): 2967, 2938, 2878, 1790, 1603, 1581, 1520, 1497, 1313, 1238, 1143, 852.

G2-AZO-C4(S). Compound **1** (0.60 g, 1.09 mmol) was dissolved in dry dichloromethane (15 mL) under an argon atmosphere. Poly(propyleneimine) dendrimer having 16 peripheral amino groups (0.10 g, 0.06 mmol) was dissolved in dry dichloromethane (10 mL) and added to the stirred solution of the pentafluorophenyl ester. On mixing the transparent solution became turbid. The mixture was stirred for 7 days and then diluted with dichloromethane (50 mL) and washed with 2% NaOH

aqueous solution (2×20 mL). The combined aqueous phases were again extracted with dichloromethane and the combined organic phases were dried over anhydrous sodium sulfate and concentrated in vacuo. The crude product was purified by flash column chromatography on silica gel using dichloromethane as eluent. The product was dissolved in the minimum amount of dichloromethane and precipitated in ethanol. Finally, the resulting material was dried at 40°C under a vacuum for 48 h. Yield: 50% (0.23 g, 0.03 mmol). ^1H NMR (400 MHz, CDCl_3 , δ): 7.81 (dd, $J = 8.8, 3.6$ Hz, 64H), 7.09–6.97 (s broad, 16H), 6.93 (d, $J = 9.0$ Hz, 32H), 6.90 (d, $J = 8.8$ Hz, 32H), 4.42–4.30 (m, 16H), 3.93 (t, $J = 5.6$ Hz, 32H), 3.27–3.13 (m, 32H), 2.72–2.35 (m, 84H), 2.23–2.11 (m, 32H), 1.85–1.53 (m, 156H), 1.50–1.38 (m, 32H), 1.31 (d, $J = 6.0$ Hz, 48H), 0.97 (t, $J = 7.4$ Hz, 48H). ^{13}C NMR (100 MHz, CDCl_3 , δ): 173.8, 160.8, 160.3, 147.0, 146.6, 124.2, 124.2, 115.7, 114.5, 75.1, 67.9, 50.9–50.2, 37.1, 36.3, 29.2, 29.0, 25.7, 25.6, 24.0–23.1, 19.3, 9.7. IR (KBr, cm^{-1}): 3293, 3072, 2937, 2870, 1645, 1600, 1580, 1498, 1247. MALDI-TOF MS (matrix: dithranol) Calcd for $\text{C}_{440}\text{H}_{624}\text{N}_{62}\text{O}_{48}$: 7550.05. Found: 7570.8. Anal. Calcd for $\text{C}_{440}\text{H}_{624}\text{N}_{62}\text{O}_{48}$: C, 70.00; H, 8.33; N, 11.50. Found: C, 69.40; H, 8.02; N, 11.25.

G3-AZO-C4(S). Compound **1** (0.77 g, 1.40 mmol) and the generation of poly(propyleneimine) dendrimer having 32 peripheral amino groups (0.14 g, 0.04 mmol) were allowed to react according to the procedure described for **G2-AZO-C4(S)**. Yield: 25% (0.15 g, 0.01 mmol). ^1H NMR (400 MHz, CDCl_3 , δ): 7.79 (dd, $J = 8.8, 3.6$ Hz, 128H), 7.44–7.27 (s broad, 32H), 6.91 (d, $J = 9.0$ Hz, 64H), 6.88 (d, $J = 8.8$ Hz, 64H), 4.40–4.27 (m, 32H), 3.92 (t, $J = 5.6$ Hz, 64H), 3.30–3.15 (m, 64H), 2.67–2.27 (m, 180H), 2.26–2.15 (m, 64H), 1.85–1.36 (m, 380H), 1.29 (d, $J = 6.0$ Hz, 96H), 0.96 (t, $J = 7.4$ Hz, 96H). ^{13}C NMR (100 MHz, CDCl_3 , δ): 173.9, 160.9, 160.3, 146.9, 146.6, 124.3, 124.2, 115.7, 114.5, 75.2, 67.9, 50.8–50.0, 37.1, 36.2, 29.1, 29.0, 25.8, 25.6, 24.0–22.9, 19.2, 9.7. IR (KBr, cm^{-1}): 3293, 3075, 2938, 2866, 1644, 1601, 1580, 1498, 1245. MALDI-TOF MS (matrix: dithranol) Calcd for $\text{C}_{888}\text{H}_{1264}\text{N}_{126}\text{O}_{96}$: 15240.32. Found: 15255.4. Anal. Calcd for $\text{C}_{888}\text{H}_{1264}\text{N}_{126}\text{O}_{96}$: C, 69.98; H, 8.36; N, 11.58. Found: C, 69.66; H, 8.24; N, 11.34.

Characterization Techniques. Elemental analyses were performed using a Perkin-Elmer 240C microanalyzer. IR spectra were obtained on a Nicolet Avatar 360-FT-IR spectrophotometer using KBr pellets. ^1H NMR and ^{13}C NMR spectra were acquired at room temperature (RT) with a Bruker AV-400 spectrometer at 400 MHz for ^1H and at 100 MHz for ^{13}C . MALDI-TOF mass spectrometry was performed on a Bruker Daltonics Autoflex apparatus using dithranol as the matrix. Thermal stability was studied by thermogravimetric analysis (TGA) under a nitrogen atmosphere using a TA Q5000IR instrument at a heating rate of $10^\circ\text{C min}^{-1}$. The mesogenic behavior was evaluated by optical microscopy using an Olympus BH-2 polarizing microscope fitted with a Linkam THMS600 hot stage. Thermal transitions were determined by DSC using a TA DSC Q-2000 instrument under a nitrogen atmosphere with powdered samples (about 3 mg) sealed in aluminum pans. Glass transition temperatures were determined at the midpoint of the baseline jump and the mesophase-isotropic phase transition temperature was read at the maximum of the corresponding peaks. X-ray diffraction (XRD) measurements were performed with an evacuated Pinhole camera (Anton-Paar) operating with a point-focused Ni-filtered Cu-K beam. Powdered samples of the azodendrimers were placed in quartz Lindemann capillaries of 1 mm diameter. The patterns were collected on flat photographic films perpendicular to the X-ray beam. Samples for AFM were prepared by casting

dichloromethane solutions of the azodendrimers (1 mg/mL) onto freshly cleaved mica. Thin film morphology was investigated by AFM (Nanoscope controller IIIa) in tapping mode with a silicon tip (spring constant about 256 kHz and force constant about 40 N/m) both in as-casted films and in films heated up to the isotropic state and quenched to RT. UV-vis and CD spectra were registered using a Jasco J-810 spectropolarimeter on either dendritic solutions or dendritic films. Film thickness was measured using a DEKTAK profilometer and values in the range of 350–500 nm were obtained for the thermally treated films. These films exhibited a good transparency and no remarkable scattering is appreciated even after thermal or optical treatment (see the Supporting Information). The CD spectra of the films were registered by rotating the samples every 60 degrees around the light beam axis in order to check that the contribution of linear dichroism to CD spectra is negligible. Films were thermally treated by annealing either in the mesophase or in the isotropic state for 5 min followed by rapid cooling to room temperature. Irradiation with unpolarized UV light was carried out using an Hg lamp (1000 W, Oriel). The wavelength ($365\text{ nm} \pm 10$) was selected using a monochromator and the film was placed at a distance of 10 cm from the monochromator. Irradiation with left-circularly polarized visible light (l-CPL) or right-circularly polarized visible light (r-CPL) was carried out using the 488 nm line of an Ar^+ laser (power 20 mW/cm^2).

Results and Discussion

1. Synthesis and Characterization of the Materials. Photochromic dendrimers **Gn-AZO-C4(S)** based on the second ($n = 2$) and third ($n = 3$) generations of PPI-derived dendrimers were synthesized by grafting the 4-[2-(S)-methylbutoxy]azobenzene units onto the periphery as shown in Scheme 1. Amidation of the amine groups was accomplished by using the activated pentafluorophenyl ester of **AZO-C4(S)**.⁴⁷ The resulting dendrimers were isolated by column chromatography and final reprecipitation from dichloromethane solutions to yield air-stable solids, which were dried under vacuum at 40°C . The resulting dendrimers have good solubility in organic solvents such as THF and chlorinated solvents. We previously undertook the synthesis of analogous poly(propylene imine) dendrimers (generation with 16 peripheral groups) functionalized with cyanoazobenzene units using hexamethylenic and decamethylenic flexible spacers. However, in those cases, we obtained materials with limited solubility in common organic solvents and this led to incomplete functionalization of the dendrimer surface, probably because of the strong interactions between the cyanoazobenzene units.²⁹ In the present work, soluble dendrimers were obtained using a hexamethylenic spacer because the alkyl terminal chains decrease intermolecular interactions between azobenzenes, leading to better solubility even with higher dendrimer generations.

The chemical structure and composition of the resulting materials was checked by several techniques, including elemental analysis, infrared spectroscopy, and NMR,

(47) Seebach, D.; Lapierre, J. M.; Skobridis, K.; Greiveldinger, G. *Angew. Chem., Int. Ed.* **1994**, 33, 440–442.

Table 1. Thermal Stability and Phase Transitions of the Azodendrimers Studied by Thermogravimetry and DSC

azodendron	TGA (°C) ^a		DSC (°C) ^b	
	<i>T</i> _{5%}	<i>T</i> _{ONSET}	cooling	heating
G2-AZO-C4(S)	150	135	I 74 (4.3) SmA 65 (15.5) C 46 g	g 50 C 81 (19.6) (SmA) I ^c
G3-AZO-C4(S)	270	300	I 110 (9.1) SmA 87 (22.3) C 60 ^d g	g 60 C 118 (32.2) (SmA) I ^c

^a *T*_{5%} and *T*_{ONSET} correspond to the temperatures at which 5% weight loss is detected and to the onset of the first weight loss, respectively.

^b Transition temperatures detected on the second cooling scan and subsequent heating. Enthalpy values are shown in brackets (J/g). ^c A short interval in which the mesophase and isotropic phase coexist is detected in the melting process (see text). ^d *T*_g is not clearly detected on cooling, but a small jump is observed at around 60 °C.

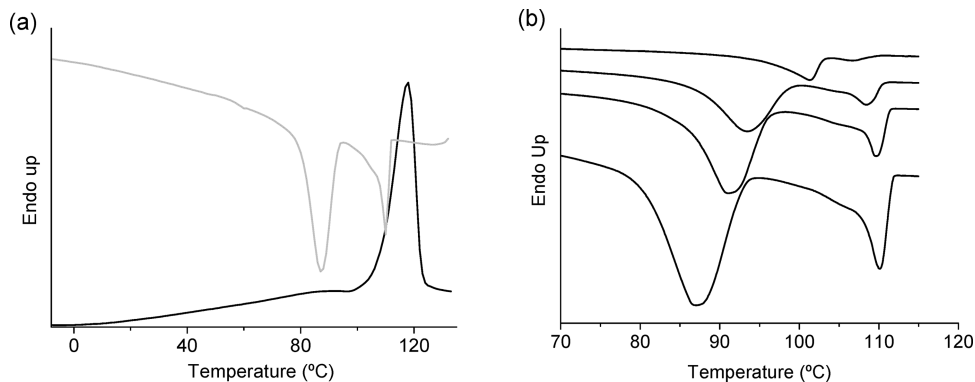


Figure 1. DSC traces: (a) corresponding to the second cooling (gray) and subsequent heating (black) processes of **G3-AZO-C4(S)** at 10 °C/min; (b) corresponding to **G3-AZO-C4(S)** cooled from the isotropic state at different rates (from bottom to top): 10, 5, 3, and 1 °C/min.

and the results corroborated the expected structures. The complete functionalization of the periphery of the dendrimer was confirmed by the absence in the ¹H and ¹³C NMR spectra of signals at δ = 2.6 and 41 ppm, respectively, corresponding to the methylene unit α to the primary amine groups of the starting dendrimer (see the Supporting Information). The complete functionalization was also checked by MALDI-TOF mass spectrometry. MALDI-TOF MS spectra revealed the presence of an intense peak corresponding to the completely functionalized dendrimer. Furthermore, a distribution of separated peaks would be expected at around 383 (molar mass of the peripheral azobenzene unit) for incomplete functionalization, but such peaks were not detected. Several small peaks were detected below the peak associated with complete functionalization and these are thought to be due to statistical defects present in the original PPI dendrimer (see the Supporting Information).⁴⁸

2. Thermal and Mesomorphic Properties of the Materials. The thermal stability of dendrimers was studied by thermogravimetric analysis under a nitrogen atmosphere. Different thermal stability behavior was observed for the two generations of dendrimers (see Table 1). The lower generation dendrimer, **G2-AZO-C4(S)**, exhibits a progressive weight loss at temperatures above 130 °C while **G3-AZO-C4(S)** shows a higher stability and the weight loss associated with thermal degradation is detected at temperatures of around 300 °C. Nevertheless, functionalization of the higher generation dendrimer leads to a material that is thermally stable up to around 300 °C. In a previous paper,²⁹ the different thermal stability of

dendrimers and codendrimers was reported to depend on the composition of these materials.

The thermal transitions and liquid crystalline behavior of the functionalized dendrimers were studied by optical microscopy, DSC, and X-ray diffraction, and the results are summarized in Table 1. Under the polarizing optical microscope the dendrimers melted to give an anisotropic fluid with an ill-defined mesomorphic texture and simultaneous isotropization was also detected. On the **G2-AZO-C4(S)** being cooled from the isotropic state (samples were heated only to 100 °C in order to avoid weight loss), the material displayed a grainy and poorly defined texture at around 75 °C that was difficult to assign. On **G3-AZO-C4** being cooled, a mesophase appeared at around 110 °C. In this case, the texture became well-defined upon short annealing at the mesophase temperature and a focal-conic texture with some homeotropic regions was observed, which is consistent with a smectic A phase (see the Supporting Information). Notable changes in the texture were not observed on cooling the samples further to RT.

DSC measurements were carried out on powdered samples at a scan rate of 10 °C/min and both dendrimers exhibited similar behavior. The heating and cooling processes (both at 10 °C/min) for **G3-AZO-C4(S)** are shown in Figure 1a as an example. In the heating process, a *T*_g is evidenced as a jump in the baseline and is followed by an endothermic peak. This peak appears in the temperature range in which the melting and isotropization of the material are detected by optical microscopy. However, two peaks were detected in the cooling process. The first peak can be assigned to the isotropic state-mesophase transition according to the optical microscopy observations. The second peak (detected before

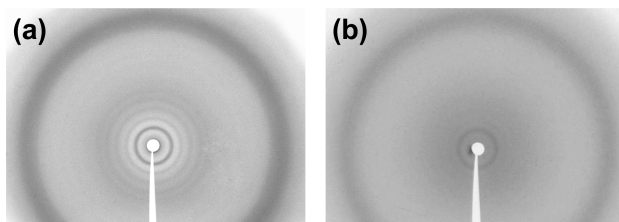


Figure 2. X-ray diffractograms of a powdered sample of **G3-AZO-C4(S)** (a) slowly and (b) quickly cooled from the isotropic state to room temperature.

vitrification) shifts toward a higher temperature if the cooling rate is decreased—as can be observed in Figure 1b. On the other hand, the total enthalpic change involved for both peaks is of the same order as that involved in the endothermic peak detected in the heating processes. Taking into account the high enthalpic content of the low temperature peak detected on cooling and its dependence on the cooling rate, it can be proposed that this peak corresponds to partial crystallization of the material. Nevertheless, crystallization can be avoided by rapid cooling, which gives rise to a glassy material. Thus, when samples were quenched from the isotropization state, the DSC trace of the subsequent heating process exhibits a cold crystallization above the T_g .

To gain an insight into the mesomorphic behavior of these materials, powdered samples of both azodendrimers cooled either slowly (0.2 °C/min) or rapidly (> 10 °C/min) from the isotropic state to RT were studied by XRD. In all cases, the patterns are consistent with a lamellar organization with a layer thickness of around 58 Å for **G3-AZO-C4(S)** and 55 Å for **G2-AZO-C4(S)**. As an example, XRD patterns corresponding to samples of **G3-AZO-C4(S)** cooled slowly or rapidly from the isotropic state are shown in Figure 2. Differences between the two types of sample (fast and slow cooling) only concern the number of orders of diffraction observed in the diffractogram and not the thickness of the lamellar organization. Diffractograms of the rapidly cooled samples (Figure 2b) are consistent with a smectic organization and only a sharp ring at low angle, corresponding to the second-order diffraction of the smectic layers, and a diffuse peak at high angle are observed. Taking into account the size of the mesogenic unit (about 22 Å considering the aliphatic spacer) a bilayer smectic A organization (vitrified mesophase) can be postulated, a proposal that is consistent with the textures observed by optical microscopy. In this mesomorphic organization, dendrimers behave as a supercalamitic cylinder with the central part occupied by the dendrimer core and the interacting mesogens elongated upward and downward with respect to the PPI dendrimeric core. As deduced from the layer thickness data, the length of this supercalamitic cylinder does not vary significantly from **G2-AZO-C4(S)** to **G3-AZO-C4(S)**, a situation described previously for other calamitic liquid crystalline dendrimers.⁴⁹ On increasing

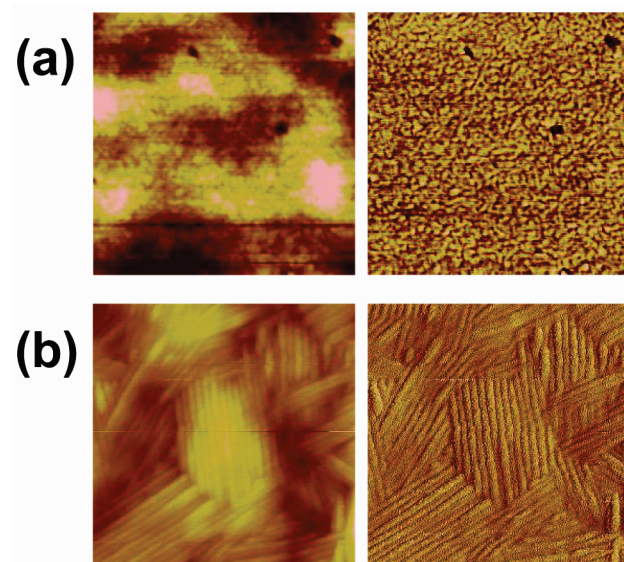


Figure 3. AFM images observed on (a) as-casted thin film surface of **G3-AZO-C4(S)** on mica and (b) after annealing at the isotropic state and quenched to RT. Topography image (left) and phase image (right) with Z range of 10 nm (topography) and 10° (phase). Image size in (a) = 1000 × 1000 nm. Image size in (b) = 400 × 400 nm.

the PPI generation, and consequently the number of peripheral mesogenic units, the diameter of the supercalamitic cylinder also increases. However, slowly cooled samples show a higher number of reflection orders (Figure 2a), which indicates a much higher correlation length in the lamellar organization—a finding that can be attributed to partial crystallization of the sample. Nevertheless, an intense diffuse peak at high angle is also observed that may be assigned to the flexible dendritic cores, which are not involved in the crystalline region.

AFM observations of films of **G3-AZO-C4(S)** were carried out on mica either on as-prepared films or films previously heated up to the isotropic state and rapidly quenched to RT. AFM measurements performed on as-casted films of the azodendrimer only displayed a grainy morphology (Figure 3a). However, thermally treated films showed a very clear topography that is characteristic of a 2D smectic-like self-assembly with a periodicity in surface of 11 ± 1 nm (Figure 3b)—a distance larger than that determined by XRD measurements, which may be due to an inclination of the smectic layers with respect to the mica surface. Consequently, it can be stated that the lamellar arrangement is caused by the thermal treatment of the thin film resulting in a smectic glass. The well-defined layering in these dendrimers results from the microphase segregation of the flexible dendritic core and the aromatic pro-mesogenic shell.

3. Chiroptical Properties and Photomodulation. The UV-vis spectra of **G2-AZO-C4(S)** and **G3-AZO-C4(S)** were measured both in dichloromethane solutions and films. As an example, the UV-vis spectrum of **G3-AZO-C4(S)** in dichloromethane (a similar spectrum was registered for **G2-AZO-C4(S)** in solution) is shown in Figure 4 along with the spectra of as-prepared films of both

(49) Baars, M.; Sontjens, S. H. M.; Fischer, H. M.; Peerlings, H. W. I.; Meijer, E. W. *Chem.—Eur. J.* **1998**, *4*, 2456–2466.

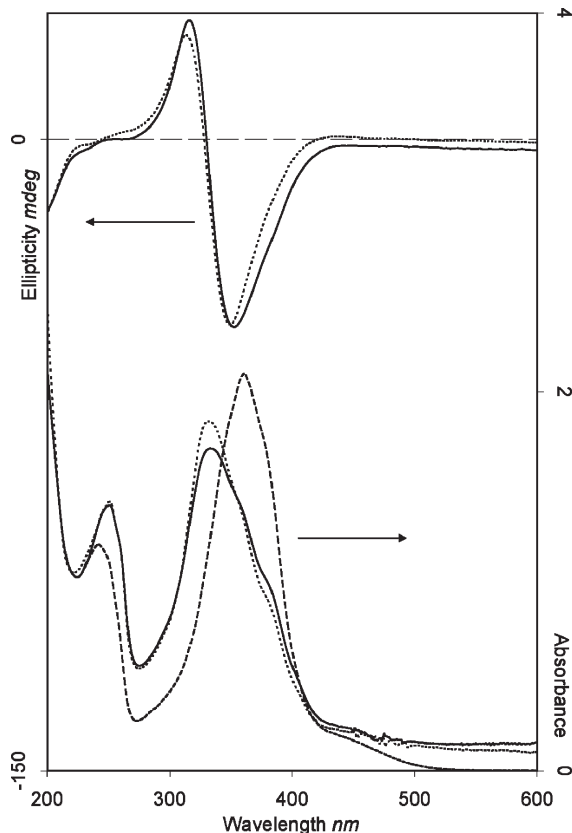


Figure 4. CD spectra of as-prepared films **G2-AZO-C4(S)** (.....) and **G3-AZO-C4(S)** (—); UV-vis spectra of as-prepared films **G2-AZO-C4(S)** (.....), **G3-AZO-C4(S)** (—), and **G3-AZO-C4(S)** in dichloromethane solution (---).

dendrimers. Dendrimers in solution show an intense absorption band at 365 nm due to the $\pi-\pi^*$ transition (A-band) of the azobenzene moiety. In addition, a weak $n-\pi^*$ transition at 450 nm and a second $\pi-\pi^*$ transition (B-band) at 245 nm can also be observed.⁵⁰ In the as-prepared films, the absorption maximum of the main $\pi-\pi^*$ transition band is shifted to shorter wavelength (from 365 to 333 nm). This behavior is caused by the supramolecular arrangement of chromophores in aggregates through $\pi-\pi$ stacking, with the blue-shifted band assigned to H-aggregates.^{51,52} This band was observed as a wide band in analogous side-chain liquid crystalline polymethacrylates having the same chiral azobenzene mesogenic unit.⁴⁵ However, the band is narrower in the dendrimeric films. This fact and the large blue-shift of the A-band of dendrimeric film spectra with respect to the solution spectra is probably due to a strong coupling of chromophores. In the literature, such types of aggregates are occasionally referred to as H*-aggregates.^{53,54} This phenomenon could be a consequence of the dendritic

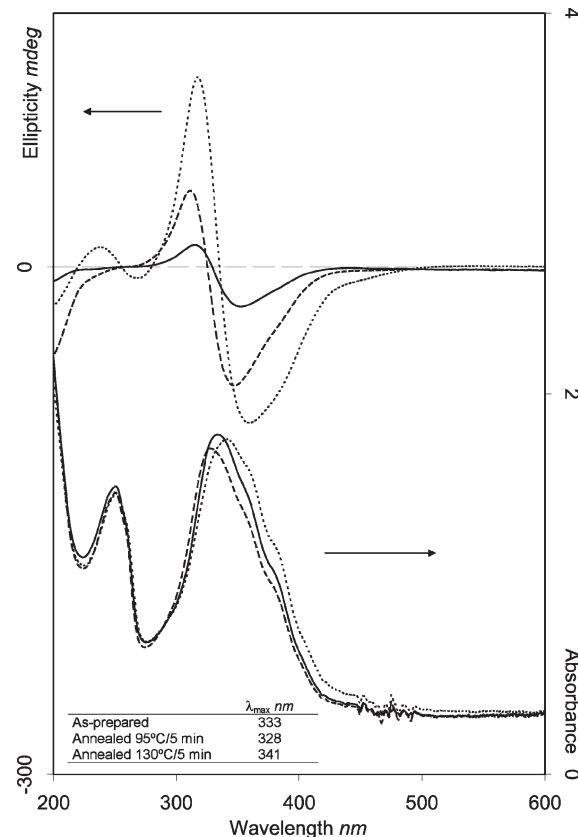


Figure 5. CD (top) and UV-vis (bottom) spectra of **G3-AZO-C4(S)**: as-prepared film (—); after annealing at 95 °C for 5 min and quenching to RT (---), and after annealing at 130 °C for 5 min and quenching to RT (.....). Inset: λ_{max} of absorbance.

structure, which facilitates an efficient interaction between azobenzene units at the periphery.

Dichloromethane solutions of the dendrimers were not CD-active. However, CD bands were clearly detected on as-prepared films of both dendrimers. The main absorption band in each of the azodendrimers is CD-active, indicating chiral supramolecular arrangements of the transition moments of the azo chromophores within the aggregates. In fact, a negative exciton couplet (a positive Cotton effect at shorter wavelength and a negative Cotton effect at longer wavelength) was observed for each azodendrimer, a finding that is indicative of a left-handed chiral organization of the transition moments of the azo units. These chiroptical supramolecular properties are driven by the molecular chirality of the terminal alkyloxy chain, which imposes a chiral arrangement of the chromophores within the aggregates.⁴⁵

Aggregation of azobenzene units can be affected by the thermal history of the film and, consequently, so can the chiroptical properties. In order to study this influence, the UV-vis and CD spectra of **G3-AZO-C4(S)** were registered for as-prepared films and films after annealing at 95 °C for 5 min (mesophase state) or 130 °C for 5 min (isotropic state) followed by quenching to RT. The spectra obtained for these samples are displayed in Figure 5. As mentioned above, the UV-vis spectrum of the as-prepared film of **G3-AZO-C4(S)** exhibits a band at 333 nm assigned to H-aggregates with strongly coupled

(50) Beveridge, D. L.; Jaffe, H. H. *J. Am. Chem. Soc.* **1966**, *88*, 1948–1953.
 (51) Kasha, M.; Rawls, H. R.; El-Bayoumi, M. A. *Pure Appl. Chem.* **1965**, *11*, 371–392.
 (52) Shimomura, M.; Ando, R.; Kunitake, T. *Ber. Bunsenges. Phys. Chem.* **1983**, *87*, 1134–1143.
 (53) Asanuma, H.; Shirasuka, K.; Takarada, T.; Kashida, H.; Komiyama, M. *J. Am. Chem. Soc.* **2003**, *125*, 2217–2223.
 (54) Narayan, G.; Kumar, N. S. S.; Paul, S.; Srinivas, O.; Jayaraman, N.; Das, S. *J. Photochem. Photobiol. A* **2007**, *189*, 405–413.

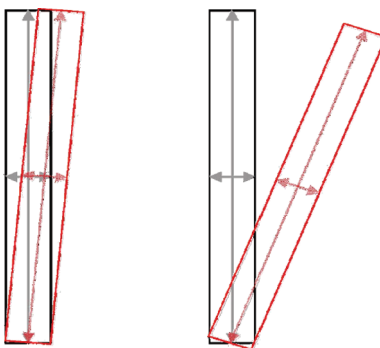


Figure 6. Schematic representations of chiral aggregates with a near parallel arrangement of electronic transition moments (left) and with a higher angle between the electronic transition moments (right).

azobenzene units. Moreover, this band displays CD activity. After annealing at the mesophase temperature (95 °C) the main band is narrower and blue-shifted to 328 nm, a change that may be related to a stronger coupling of the azo chromophores within aggregates. In addition, the CD amplitude increases and the crossover of this band is also blue-shifted. As explained above, the smectic organization of LC dendrimers can be understood in terms of a supermolecule adopting a cylindrical conformation with peripheral mesogenic units approximately parallel to each other.^{55,56} The observed CD results can be explained by the smectic order imposing a compact assembly of azobenzene mesogenic units with slightly rotated (near parallel) chromophore transition moments (Figure 6). This slight rotation is responsible for the amplified supramolecular chirality, which is ultimately governed by the stereocenters incorporated in the terminal alkyl chains.⁵⁷

The annealing process in the isotropic state (130 °C) produces a red shift and a broadening of the main band along with an unexpected increase in the CD amplitude. Moreover, a new exciton couplet associated with the $\pi-\pi^*$ dipolar transition moments along the short axis of the azo chromophore (B band) was also detected. It must be taken into account that quenching from the isotropic state to RT results in smectic glasses according to the X-ray diffraction and AFM data. Bearing this in mind, the results can be explained if we consider that quenching from the isotropic state precludes a good packing of the azobenzene units within the smectic A layers. In other words, the dendritic supermolecules tend to be approximately parallel to each other, giving rise to the smectic layer, but the azobenzene units are less strongly coupled and less parallel than in the case of films annealed at the mesophase temperature. As a consequence, the main $\pi-\pi^*$ transition (A band) is broader and red-shifted. The angle between the electronic transition moment along the long axes increases, as does the

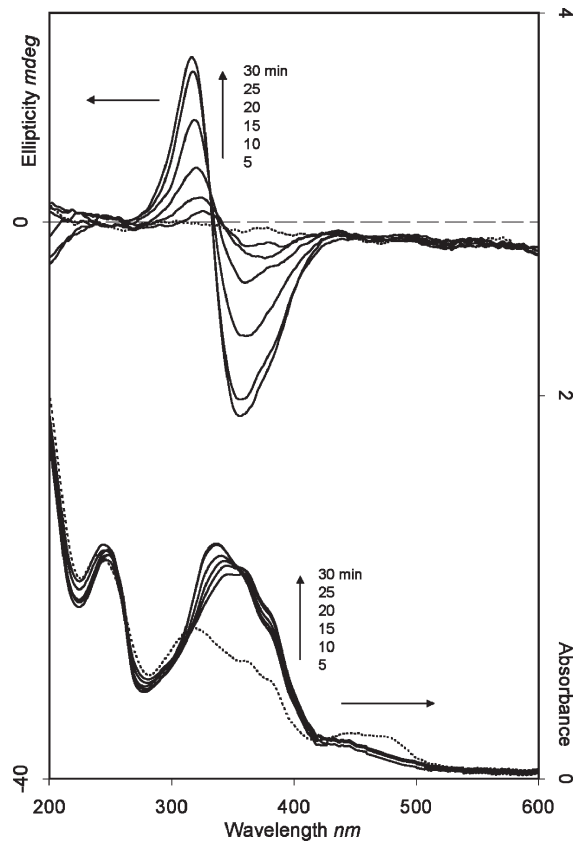


Figure 7. CD (top) and UV-vis (bottom) spectra of G3-AZO-C4(S) after irradiation at 365 nm for 5 min (....) and after showed time exposed at visible light at RT (—).

CD response of the main band. Besides, the angle between the electronic transition moments along the short axes (B band) increases sufficiently to cause an exciton couplet of the B band, as it is schematically represented in Figure 6.^{58,59}

With the aim of studying the effect of the trans-cis-trans isomerization of azobenzene moieties on the aggregation behavior, an annealed film (130 °C, 5 min and quenched to RT) of G3-AZO-C4(S) was irradiated with UV light (irradiation wavelength = 365 nm). A photo-stationary state was reached in 5 min. A decrease in the optical absorption is observed in the region of the $\pi-\pi^*$ band together with an increase in the $n-\pi^*$ band region attributed to the trans-cis isomerization process, a well-known phenomenon for azobenzenes. UV irradiation (and the subsequent trans-cis isomerization) also led to the erasure of the chiroptical properties as a consequence of the disappearance of chiral supramolecular aggregates of trans azobenzenes. The sample was left standing at RT (cis-trans back isomerization) and the UV-vis and CD spectra were registered at different times until variation of the spectra was no longer evident (Figure 7). Two processes were detected during this time. The first one is the expected cis-trans back isomerization. After 5 min, the UV spectrum of the trans isomer was recovered but only a

(55) Barberá, J.; Donnio, B.; Gehringer, L.; Guillou, D.; Marcos, M.; Omenat, A.; Serrano, J. L. *J. Mater. Chem.* **2005**, *15*, 4093–4105.

(56) Marcos, M.; Martin-Rapun, R.; Omenat, A.; Serrano, J. L. *Chem. Soc. Rev.* **2007**, *36*, 1889–1901.

(57) Percec, V.; Imam, M. R.; Peterca, M.; Wilson, D. A.; Graf, R.; Spiess, H. W.; Balagurusamy, V. S. K.; Heiney, P. A. *J. Am. Chem. Soc.* **2009**, *131*, 7662–7677.

(58) Berova, N.; Di Bari, L.; Pescitelli, G. *Chem. Soc. Rev.* **2007**, *36*, 914–931.

(59) Nakashima, N.; Morimitsu, K.; Kunitake, T. *Bull. Chem. Soc. Jpn.* **1984**, *57*, 3253–3257.

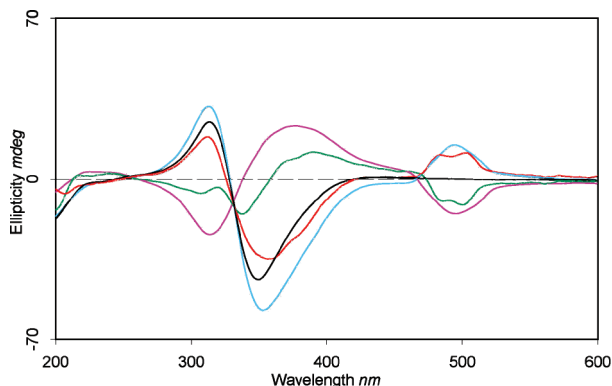


Figure 8. CD and UV-vis spectra of **G2-AZO-C4(S)** as-prepared film (black); l-CPL irradiated (blue); a month after l-CPL irradiation (red); r-CPL irradiated (purple); and a month after r-CPL irradiation (green).

weak CD signal was detected, i.e., the recovery of the chiral assembly is not simultaneous with the cis-trans back isomerization of the azo units. The second process is the aggregation of trans azobenzenes, which is detected as a blue-shift of the $\pi-\pi^*$ band in the UV spectrum as reported previously by other authors.⁶⁰ Furthermore, in our case, an increase of the CD signal due to supramolecular chirality is also observed as a consequence of the recovery of the chiral aggregation. Consequently, chiroptical properties can be easily erased and recovered in these films through trans-cis-trans isomerization and aggregation.

Irradiation with a chiral light source (i.e., circularly polarized light, CPL) of azobenzene units may induce or modify the chiroptical properties associated with chiral supramolecular entities in azopolymers. In this sense, we previously corroborated that the irradiation with CPL of achiral side-chain liquid crystalline azopolymers induced a chiral arrangement that depends on the handedness of the light.^{43,44} Furthermore, the supramolecular chirality of chiral liquid crystalline azopolymers can be controlled by irradiation with CPL.⁶¹ To analyze how irradiation with CPL can modulate the supramolecular chirality induced by stereocenters, as-prepared dendrimeric films were irradiated with left or right circularly polarized light (l-CPL or r-CPL) at 488 nm (Ar^+ laser, 20 mW/cm²) for 30 min. The results obtained for **G2-AZO-C4(S)** are shown in Figure 8. As can be seen, irradiation with l-CPL reinforces the CD supramolecular response imposed by the stereocenters in that dendrimer. Furthermore, a positive nonabsorptive signal appears at around 490 nm, probably due to a selective reflection.^{41,44} The CD response of the film irradiated with l-CPL remains after leaving the film for one month at RT. However, irradiation with r-CPL switches the chiroptical properties. The CD spectrum of the film irradiated with r-CPL shows a positive exciton couplet corresponding to the $\pi-\pi^*$ band, with the crossover shifted to a longer wavelength. Furthermore, a negative nonabsorptive signal at around

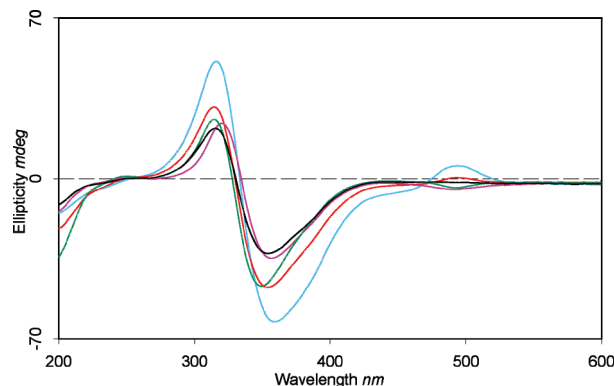


Figure 9. CD and UV-vis spectra of **G3-AZO-C4(S)** as-prepared film (black); l-CPL irradiated (blue); a month after l-CPL irradiation (red); r-CPL irradiated (purple); and a month after r-CPL irradiation (green).

490 nm was also observed. When films irradiated with r-CPL were left at RT in darkness for a month, evolution of the chiroptical properties was detected. Exciton couplet evolves from positive to negative, the original sense determined by stereocenters.

The results corresponding to **G3-AZO-C4(S)** films are shown in Figure 9. In a similar way to **G2-AZO-C4(S)**, irradiation of a **G3-AZO-C4(S)** film with l-CPL reinforces the supramolecular chirality imposed by stereocenters and induces a slight nonabsorptive signal at around 490 nm. The increase in the CD intensity is partially maintained after a month at room temperature. However, the most significant result is obtained upon irradiation of a **G3-AZO-C4(S)** film with r-CPL. In contrast to the change observed for **G2-AZO-C4(S)**, switching of the chiroptical properties was not detected by irradiation with r-CPL under the same irradiation conditions. Irradiation time was also increased up to 60 min, but no changes were observed in the CD spectrum. No switching was also observed in **G3-AZO-C4(S)** if derived films are irradiated for 30 min at 488 nm with a higher intensity (40 mW/cm²). This result contrasts with that obtained in previous studies dealing with amorphous and liquid crystalline chiral azopolymers having a side-chain architecture, which showed a net inversion of sign of the CD signal under irradiation with one-handed circularly polarized (the other one reinforces the original CD signal).⁶¹⁻⁶⁴ This fact puts in evidence the influence of the dendrimeric architecture. The anisotropic phases of liquid crystalline dendrimers are the result of the competition between the tendency of the branches to be isotropically distributed in the space because of the entropic forces and the strong interactions between peripheral mesogenic units, which produce an enthalpic gain. As mentioned above, a model to explain the smectic organization in dendrimers considers that these compounds adopt a cylindrical conformation (calamitic supermolecule),

(60) Meier, J. G.; Ruhmann, R.; Stumpe, J. *Macromolecules* **2000**, *33*, 843-850.

(61) Barberá, J.; Giorgini, L.; Paris, F.; Salatelli, E.; Tejedor, R. M.; Angiolini, L. *Chem.—Eur. J.* **2008**, *14*, 11209-11221.

(62) Angiolini, L.; Giorgini, L.; Bozio, R.; Pedron, D. *Synth. Met.* **2003**, *138*, 375-379.

(63) Angiolini, L.; Bozio, R.; Giorgini, L.; Pedron, D.; Turco, G.; Daurù, A. *Chem.—Eur. J.* **2002**, *8*, 4242-4247.

(64) Angiolini, L.; Benelli, T.; Bozio, R.; Daurù, A.; Giorgini, L.; Pedron, D. *Synth. Met.* **2003**, *139*, 743-746.

with the mesogenic units arranged approximately parallel to each other. On increasing the generation number, a larger number of mesogenic units must be accommodated in the cylinder^{55,56} and these are forced to interact. This situation hinders the switching of the original supramolecular chiral organization, as in the case of that **G2-AZO-C4(S)**, or eventually prevents the switching altogether as the generation number increases [dendrimer **G3-AZO-C4(S)**].

Conclusions

Two new liquid crystalline dendrimers containing azo chromophores with chiral terminal chains have been synthesized and characterized. The dendrimers exhibit a smectic phase that can be frozen at RT depending on the thermal history of the sample. Azobenzene units tend to form aggregates in solid films. A study of chiroptical properties of these materials revealed that the stereocenters of the terminal chains imposed a supramolecular chirality associated with azobenzene aggregation, which is responsible for the CD response detected in the dendritic films. Furthermore, this response varies slightly with the thermal history of the sample. By irradiation with UV-light (trans–cis isomerization) chiroptical properties can be erased and recovered again by leaving the sample at RT (cis–trans back isomerization and

aggregation). For these materials, it has been shown that the modulation of chiroptical properties with circularly polarized light (488 nm) depends on the azodendrimer generation. In the lowest generation, a switching from the stereocenter-determined CD signal to the opposite one is achieved. However, in case of the highest generation, the dense packing of azobenzenes linked at the periphery prevents the switching. These properties open the possibility of using these materials in the design of new chiroptical switches.

Acknowledgment. This work was supported by the MI-CINN, Spain, under Project MAT2008-06522-C02, FEDER fundings, Fondo Social Europeo and Gobierno de Aragón (Departamento de Ciencia, Tecnología y Universidad). J.d. B. acknowledges his grant from DGA (Gobierno de Aragón). The authors acknowledge to Dr. Joaquín Barberá for helpful discussions about X-ray measurements and Jordi Díaz of the Serveis Científicotècnics-Universidad de Barcelona for AFM measurements.

Supporting Information Available: ¹H NMR spectra and textures of **G3-AZO-C4(S)**, MALDI mass spectra of **G2-AZO-C4(S)** and **G3-AZO-C4(S)**, as well as a photograph of thick films of **G3-AZO-C4(S)** to give an impression of the light scattering properties of the quenched films (PDF). This material is available free of charge via the Internet at <http://pubs.acs.org>.